Journal of Materials Science and Chemical Engineering, 2026, 14(4), 20-30
https://www.scirp.org/journal/msce
ISSN Online: 2327-6053
ISSN Print: 2327-6045

In-Situ Synthesis of Nb_2O_5-NbC Heterojunctionsregulates the Hydrogen Storage Performance of MgH_2

Hui Zhang

School of Chemical Engineering and Pharmacy, Wuhan Institute of Technology, Wuhan, China
Email: excellentrs@163.com

How to cite this paper: Zhang, H. (2026) *In-Situ* Synthesis of Nb_2O_5-NbC Heterojunctionsregulates the Hydrogen Storage Performance of MgH_2. *Journal of Materials Science and Chemical Engineering*, **14**, 20-30.
https://doi.org/10.4236/msce.2026.144002

Received: March 22, 2026
Accepted: April 20, 2026
Published: April 23, 2026

Abstract

Among diverse hydrogen storage materials, magnesium hydride (MgH_2) is a promising solid-state candidate featuring high hydrogen capacity and low cost. However, its sluggish dehydrogenation kinetics and high initial dehydrogenation temperature drastically limit the large-scale commercialization and practical application of MgH_2. This work focuses on breaking the dehydrogenation kinetic barrier via designing a unique heterostructure catalyst to reduce desorption temperature and improve hydrogen storage performance. Ultrafine Nb_2O_5-NbC heterojunctions evenly dispersed in carbon nanofiber (CNF) matrix were synthesized through a simple electrospinning method, where polystyrene (PS) acted as a growth regulator to prevent nanoparticle agglomeration. Experimental and theoretical results demonstrate that higher electrospinning speed enlarges CNF diameter, lowering Nb_2O_5-NbC heterojunction density per unit matrix and increasing the initial desorption temperature of MgH_2 composite. Relative to neat ball-milled MgH_2, the MgH_2 composite modified by Nb_2O_5-NbC/CNF-PS catalyst shows 52.6˚C decline in initial dehydrogenation temperature and 29.1˚C drop in peak desorption temperature. The enhanced dehydrogenation performance is mainly attributed to the synergistic catalysis of Nb_2O_5-NbC heterojunctions. Moreover, the CNF matrix serves as a confinement scaffold to stabilize heterojunction nanoparticles and provides auxiliary catalytic activity, further elevating the overall hydrogen storage properties of MgH_2.

Keywords

Nb_2O_5-NbC, MgH_2, Heterojunctions, Hydrogen Storage

1. Introduction

Air pollution and global warming are plaguing the Earth. Developing clean energy

and striving to achieve zero carbon emissions have become one of the solutions adopted by countries worldwide [1]. Hydrogen is regarded as a clean and sustainable renewable energy source [2]. However, for the large-scale market application of hydrogen energy, the safety and efficiency of hydrogen storage remain critical issues that need attention [3]. Magnesium hydride (MgH_2) boasts a high hydrogen storage capacity (~7.6 wt.% and 109 kg/m^3), and magnesium resources are abundantly available [4]-[6]. Nevertheless, in practical applications, MgH_2 suffers from sluggish reactions due to the inertness of the magnesium surface, requiring high temperatures of 300˚C - 400˚C for its hydrogen absorption and desorption processes.

Currently, researchers worldwide have found that introducing transition metals (such as titanium, niobium, vanadium, cobalt, nickel, manganese, etc.) and their compounds into MgH_2 can improve the reaction kinetics and thermodynamics of MgH_2, thereby enhancing its hydrogen storage performance [7]-[9]. For example, the introduction of Nb_2O_5 into MgH_2 significantly enhances the desorption kinetics, exhibiting high catalytic activity [10]-[14]. Studies have shown that when the high-valent Nb (+5) in Nb_2O_5 is reduced to low-valent Nb (such as NbO_2, NbO, etc.), the hydrogen absorption and desorption properties of MgH_2 are significantly improved [15] [16]. This is because the multivalent Nb species uniformly dispersed in MgH_2 act as hydrogen channels and promote hydrogen diffusion [17]. In 2020, the team led by Professor Yongfeng Liu from the Laboratory of Silicon Materials at Zhejiang University used Nb_2O_5 hollow spheres (o-Nb_2O_5) to reduce the initial dehydrogenation temperature of MgH_2 to 195˚C, and more than 5.5 wt.% of H_2 could be desorbed within 5 minutes at 300˚C [14].

To further improve the hydrogen storage performance of MgH_2, various dual transition metal ions have been developed to leverage their role in weakening the Mg-H bond binding energy. For instance, under the synergistic effect of dual transition metals in $TiVO_{3.5}$, $CuFe_2O_4$, and $NiFe_2O_4$ [16] [19] [20], reactions between metal oxides and MgH_2 generate low-valent oxides or zero-valent metallic elements, increasing catalytic active sites and enhancing the hydrogen storage performance of MgH_2. In addition to dual-transition-metal catalysts, researchers have also studied the addition of various carbon nanomaterials. For example, Zou from Shanghai Jiao Tong University *et al.* used porous carbon nanofibers (pCNF) to self-assemble a scaffold of MgH_2/Ni nanoparticles (NPs), enabling MgH_2 to absorb hydrogen at 100˚C with a capacity of 2.2 wt.% within 120 minutes [20].

Liu *et al.* [21] synthesized bamboo-like carbon nanotubes for the self-assembly of MgH_2 nanoparticles, which desorbed hydrogen at approximately 220˚C with a hydrogen capacity of 5.79 wt.%. Nobuko Hanada *et al.* from Waseda University synthesized a MgH_2-Nb_2O_5-CNT composite, which desorbed 5.7 wt.% of hydrogen at 350˚C for 60 minutes [22]. Lan *et al.* [23] from Guangxi University synthesized an N-Nb_2O_5@Nb_2C-doped MgH_2 composite that started desorbing hydrogen at 178˚C and released 6.3 wt.% of hydrogen within 1.95 minutes at 350˚C. These studies have all found that CNT samples show considerable improvements

in hydrogen absorption and desorption properties. Thus, it is concluded that CNT samples exhibit higher hydrogen capacity and faster kinetics, facilitating the entry of hydrogen atoms into the interior of Mg particles and their escape.

This paper reports the synthesis of Heterojunctions Nb_2O_5-NbC uniformly distributed in a carbon nanofiber matrix. Polystyrene (PS) is introduced as a growth regulator for the Heterojunctions to control the Nb_2O_5-NbC nanocrystals and prevent agglomeration of Nb_2O_5-NbC nanocrystal particles. The *in-situ* formed Nb_2O_5-NbC Heterojunctions provides abundant active surfaces and interfacial active sites, weakening the interaction between Mg-H bonds and extending the length of Mg-H bonds. The results show that the initial desorption temperature of MgH_2 catalyzed by the Nb_2O_5-NbC Heterojunctions is reduced to 293.6˚C, 52.6˚C lower than that of ball-milled MgH_2.

The presence of NbC and Nb_2O_5 inhibits the grain size of MgH_2, providing more active centers and hydrogen diffusion paths. On the other hand, increasing the spinning speed leads to a larger diameter of carbon nanotubes, resulting in a reduction of Nb_2O_5-NbC Heterojunctionsper unit area of the carbon nanofiber matrix. This increases the kinetic barrier, leading to an increase in the initial desorption temperature of MgH_2. However, the above two inferences are speculative interpretations derived from experimental results and literature data, and do not necessarily represent the actual reaction mechanism or situation. The findings of this study provide insights for further improving the hydrogen storage performance of Mg-based hydrogen storage systems.

2. Experimental

2.1. Sample Preparation

Polyacrylonitrile, niobium oxalate and polystyrene are analytical grade, which are purchased from Sigma-Aldrich, Macklin and Alfa Aesar respectively. Dimethylformamide was purchased from Sigma. All chemical reagents are used directly after purchase. The water involved in the experiment is distilled water.

Nb_2O_5-NbC/CNF-PS [24] was synthesized according to literature reports. The overall preparation process is as follows: firstly, 1.0 g of polyacrylonitrile, 0.5 g of niobium oxalate, 0.5 g of polystyrene are dissolved in 10ml of dimethylformamide, and then stirred at 60˚C for 24 hours. Then, the electrospinning solution was put into a 10 ml plastic syringe equipped with No.21 stainless steel needle, and the feed rate was 0.035 mm/min^{-1}. In the process of electrospinning, the electrospinning solution was placed at a high voltage of 22 kV, and the obtained nanofibers were collected on a copper collector 20 cm away from the needle tip. The collected electrospun films were dried at 280˚C for 2 hours, then annealed at 900˚C for 2 hours at a heating rate of 5˚C/min in a nitrogen atmosphere.Following the feeding method of Sample ①, experiments with feed rates of 0.070 mm/min and 1.05 mm/min were designed separately, yielding Sample ② and Sample ③, respectively. The subsequent preparation procedures for Samples ②-③ were consistent with those of Sample ①: first drying at 280˚C for 2 hours, followed by annealing

at 900˚C for 2 hours in a nitrogen atmosphere with a heating rate of 5˚C/min.

Preparation of MgH_2-Nb_2O_5-NbC/CNF-PS: Nb_2O_5-NbC/CNF-PS Heterojunctions was doped into MgH_2 at 10.00 wt.% of the total mass, with MgH_2 accounting for 90 wt.% of the total mass. Samples were sealed in a grinding jar (150 mL) made of SUS304 steel inside a glove box. Stainless steel balls with diameters of 10, 5, 2 mm were used in the grinding jar. Mechanical grinding was conducted for 12 hours using a QM-3SP2 planetary ball mill (manufactured in Nanjing). The mass ratio of powder to grinding balls was approximately 120:1, and the grinding speed was 500 rpm.

To prevent sample temperature, rise due to excessive grinding speed, the ball mill rotated forward for 30 minutes, paused for 5 minutes, and then rotated backward for 30 minutes. The obtained sample was denoted as MgH_2-10 wt.% (Nb_2O_5-NbC/CNF-PS). All sample operations were performed in a glove box with a circulating purification system filled with high-purity argon (99.999%), where the water and oxygen contents were both below 0.01 ppm to prevent sample oxidation and contamination. For comparison, pure ball-milled MgH_2 was also sealed and ball-milled under the same conditions.

2.2. Structural Characterization

The phase composition of all materials was characterized by X-ray diffraction (XRD, D8 Advance, Bruker AXS) using filtered Cu Kα radiation. The detection angle 2θ ranged from 20˚ to 80˚ with a step size of 0.02˚. A field-emission scanning electron microscope (FE-SEM; JEOL7500FA, Tokyo, Japan) was used for observation.

2.3. Property Evaluation

The temperature-dependent hydrogen desorption behavior was measured using a self-made temperature-programmed desorption (TPD) system. Approximately 20 - 30 mg of the sample was loaded into a stainless-steel tubular reactor, which was then connected to the TPD system. The sample was gradually heated from room temperature to 450˚C at a rate of 2˚C/min. Typically, 20 - 30 mg of the sample was placed in the stainless-steel tubular reactor, with a thermocouple inserted into the reactor to monitor the real-time sample temperature. Hydrogen desorption was conducted in a non-isothermal mode, where the sample was heated at a heating rate of 2˚C/min under primary vacuum until complete hydrogen release. The temperature-programmed desorption (TPD) system was calibrated using standard pure hydrogen gas. The hydrogen storage capacity was calculated based on the ideal gas state equation and the sample mass. The initial desorption temperature was defined as the temperature at which the hydrogen desorption amount began to increase significantly, while the peak desorption temperature was the temperature corresponding to the maximum desorption rate. All temperature-programmed desorption experiments were repeated at least twice to ensure the reproducibility and reliability of the results.

3. Results

3.1. Preparation of Nb_2O_5-NbC/CNF-PS Heterojunctions

Nb_2O_5-NbC/CNF-PS heterojunctions were fabricated via electrospinning combined with high-temperature calcination under nitrogen atmosphere, using polystyrene as a nanocrystal growth regulator (Figure 1). The preparation procedure was as follows: niobium oxalate, polyacrylonitrile, and polystyrene were stirred at 80˚C for 24 h to achieve uniform dissolution in dimethylformamide. The precursor solution was electrospun at three feeding rates: 0.035 mm/min (Sample ①), 0.070 mm/min (Sample ②), and 1.05 mm/min (Sample ③). The as-spun fibrous film was pre-oxidized at 280˚C (heating rate: 5˚C/min) in air, then calcined at 900˚C at the same heating rate under nitrogen protection, followed by natural cooling to obtain the final composite sample.

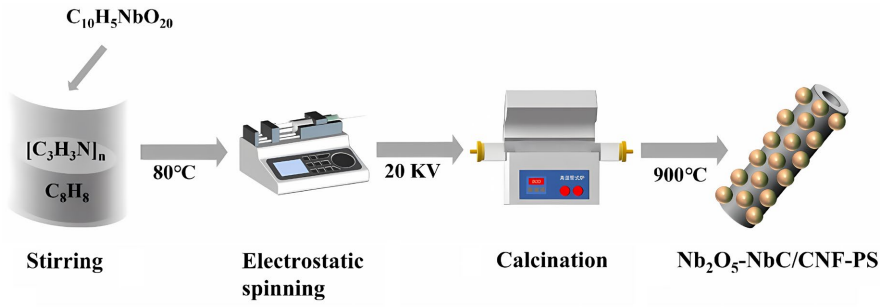

Figure 1. Schematic illustration of the synthesis strategy for ultrafine Nb_2O_5-NbC/CNF-PS.

For temperature-programmed desorption (TPD) tests, 20 - 30 mg of each sample was loaded into a stainless-steel tubular reactor in a glove box, with a thermocouple inserted to monitor sample and furnace temperatures. TPD tests were performed under vacuum (initial pressure < 0.0001 bar) with a heating rate of 2˚C/min to the preset target temperature.

3.2. XRD Analysis of Nb_2O_5-NbC/CNF-PS Heterojunctions

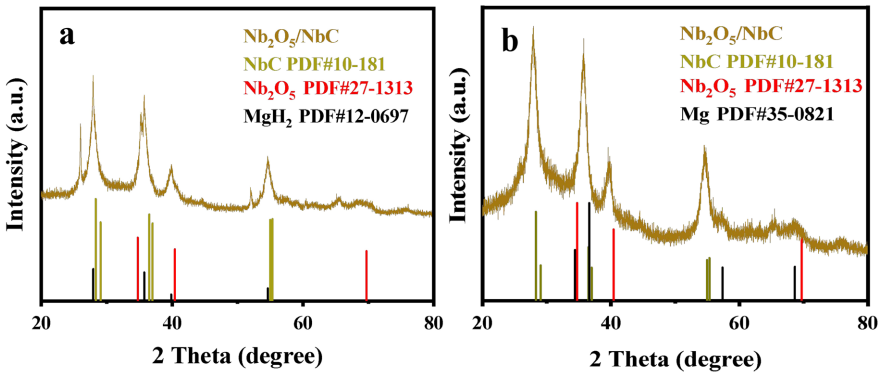

Figure 2. (a), (b) MgH_2-10 wt.% (Nb_2O_5-NbC/CNF-PS) after ball milling and after hydrogen desorption.

XRD characterization was conducted on the as-prepared Nb_2O_5-NbC/CNF-PS catalyst (Figure 2). Characteristic diffraction peaks located at 34.74˚, 40.41˚, 58.36˚, and 69.7˚ were detected, matching the standard card of NbC (PDF#00-10-181). Diffraction peaks at 28.31˚, 29.06˚, 36.49˚, 37˚, 54.97˚, and 55.33˚ were also observed, corresponding to the standard pattern of Nb_2O_5 (PDF#00-27-1313). After ball milling: the composite consists of MgH_2, Nb_2O_5, NbC. After dehydrogenation: the main phases are Mg, Nb_2O_5, NbC. The results confirm that the Nb_2O_5/NbC heterojunction is well maintained during the dehydrogenation process, which supports our conclusion.

3.3. SEM Morphology of Nb_2O_5-NbC Heterojunctions

SEM characterization was performed on the precursor samples before calcination. All three samples displayed uniform fibrous structures. For Sample ① (0.035 mm/min), the carbon nanofibers were thin, with a diameter range of 80-150 nm (Figure 3(a), Figure 3(b). Sample ② (0.070 mm/min) exhibited thicker fibers with a diameter range of 150-230 nm (Figure 3(b), Figure 3(d). Sample ③ (1.05 mm/min) possessed the thickest fibers, with a diameter range of 800-1000 nm (Figure 3(c), Figure 3(f)). All samples showed hollow fibrous structures.

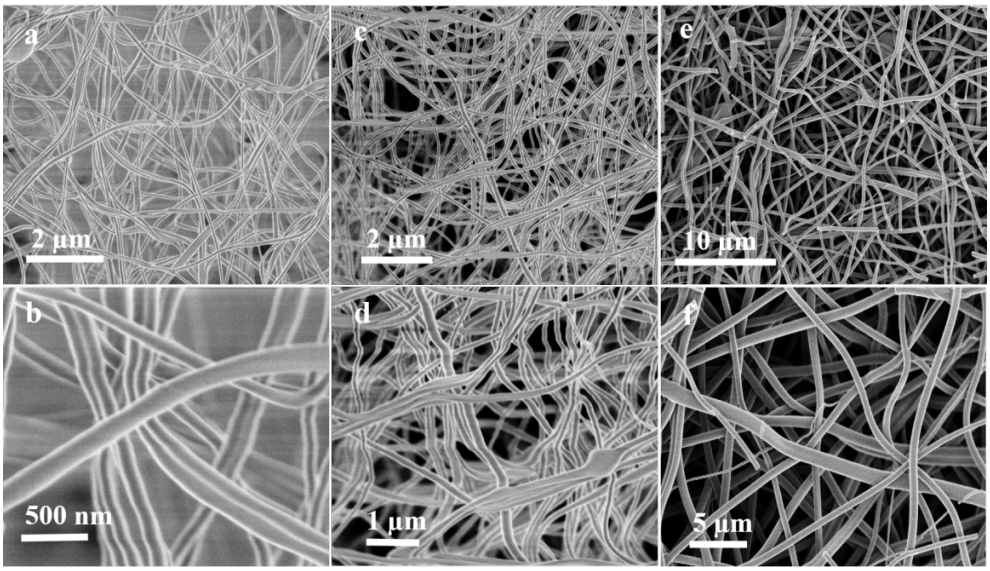

Figure 3. (a) (c) (e) and (b) (d) (f) SEM images of as-synthesized Nb_2O_5-NbC/CNF-PS at different spinning speeds before calcination.

After high-temperature calcination, the morphology of Nb_2O_5-NbC/CNF-PS composites was further observed by SEM. Nb_2O_5-NbC particles were embedded in the carbon fiber skeleton. Sample ① showed an ordered carbon fiber skeleton with uniformly dispersed Nb_2O_5-NbC particles (Figure 4(a), Figure 4(b)). Sample ② presented a relatively disordered fiber skeleton with slight particle agglomeration (Figure 4(c), Figure 4(d)). Sample ③ had a messy fiber skeleton with severe particle agglomeration and large bare fiber areas (Figure 4(e), Figure 4(f)).

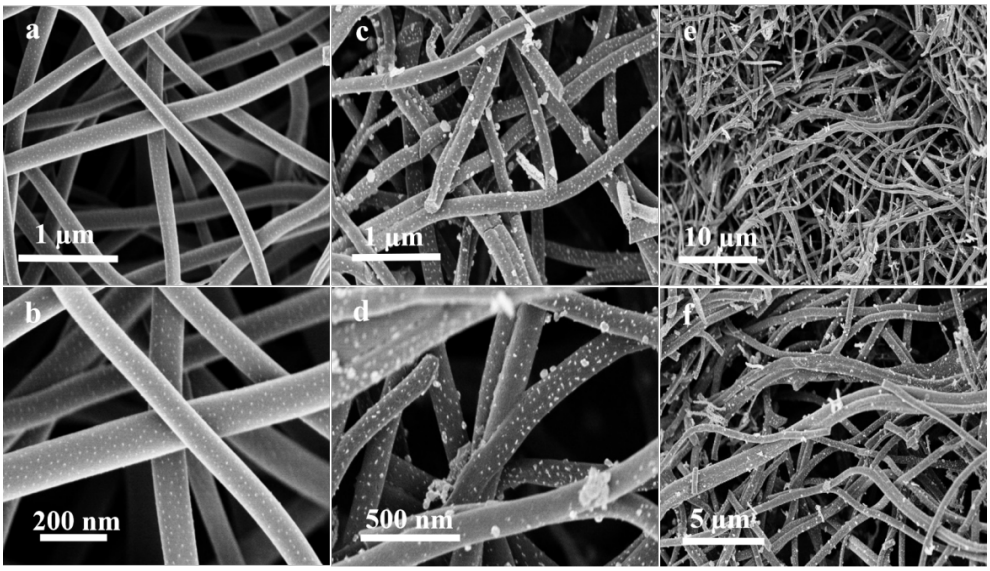

Figure 4. (a) (c) (e) and (b) (d) (f) SEM images of as-synthesized Nb_2O_5-NbC/CNF-PS at different spinning speeds after calcination.

3.4. Hydrogen Desorption Performance of MgH_2 Catalyzed by Nb_2O_5-NbC/CNF-PS Heterojunctions

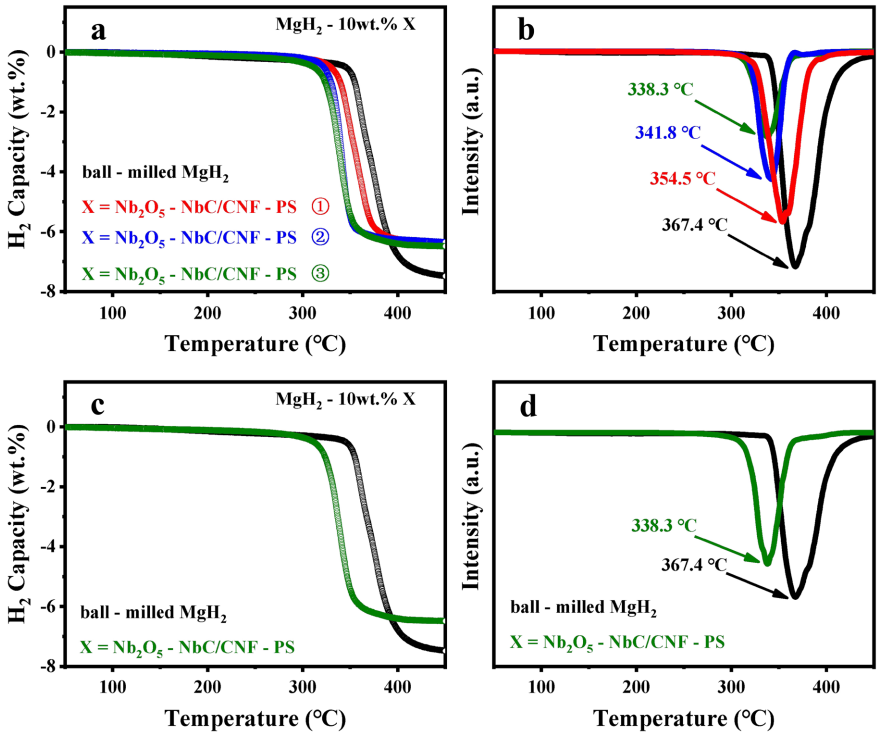

Figure 5. (a) TPD curves of MgH_2 under the catalysis of Nb_2O_5-NbC/CNF-PS at different spinning speeds, including ball-milled MgH_2. (b) The derivative curves of H_2 desorption of Nb_2O_5-NbC/CNF-PS at different spinning speeds, including ball-milled MgH_2. (c) TPD curves of MgH_2 under the catalysis of Nb_2O_5-NbC/CNF-PS at 0.035 mm/min spinning speeds, including ball-milled MgH_2. (d) The derivative curves of H_2 desorption of Nb_2O_5-NbC/CNF-PS at 0.035 mm/min spinning speeds, including ball-milled MgH_2.

TPD tests were carried out to evaluate the hydrogen desorption performance of pure ball-milled MgH_2 and MgH_2-10 wt.% (Nb_2O_5-NbC/CNF-PS) composites. All samples were heated to 450˚C at 2˚C/min under vacuum, and the corresponding TPD curves and derivative curves were recorded (**Figure 5**).

For pure ball-milled MgH_2, the initial hydrogen desorption temperature was 346.2˚C, and the hydrogen desorption capacity at 450˚C was 7.48 wt.%. For the catalyzed samples, the initial desorption temperatures were 293.6˚C (Sample ①), 302.9˚C (Sample ②), and 320.2˚C (Sample ③), with hydrogen desorption capacities of 6.48 wt.%, 6.38 wt.%, and 6.35 wt.% at 450˚C, respectively.

The hydrogen desorption peak temperatures derived from TPD curves were 367.4˚C for pure MgH_2, 338.3˚C for Sample ①, 341.8˚C for Sample ②, and 354.5˚C for Sample ③. Compared with pure MgH_2, Sample ① showed a 52.6˚C reduction in initial desorption temperature and a 29.1˚C reduction in desorption peak temperature. At 346.2˚C, the MgH_2-10 wt.% (Nb_2O_5-NbC/CNF-PS) composite released over 4.89 wt.% of H_2, while pure MgH_2 just initiated hydrogen desorption.

4. Discussion

The XRD results confirmed the successful fabrication of Nb_2O_5-NbC heterojunctions via electrospinning and high-temperature calcination, with the characteristic peaks of both Nb_2O_5 and NbC clearly detected without impurity phases. This heterostructure is critical for the subsequent catalytic modification of MgH_2, as the synergistic effect between Nb_2O_5 and NbC has been proven to effectively boost the hydrogen storage kinetics of Mg-based materials.

SEM observations revealed that the electrospinning feeding rate exerted a significant influence on the diameter and dispersion of the carbon nanofibers, as well as the distribution of Nb_2O_5-NbC particles. With the increase of feeding rate, the fiber diameter increased sharply from 80 - 150 nm to 800 - 1000 nm, accompanied by aggravated particle agglomeration and disordered fiber skeleton. This morphological evolution is attributed to the excessive solution supply at higher feeding rates, which hinders the uniform stretching of fibers during electrospinning and leads to uneven nucleation and growth of heterojunction particles during calcination. The reduced specific surface area and fewer active sites caused by particle agglomeration directly weakened the catalytic efficiency of the composite, which was consistent with the deteriorating hydrogen desorption performance of Samples ② and ③.

The hydrogen desorption data demonstrated that doping Nb_2O_5-NbC/CNF-PS heterojunctions significantly lowered the hydrogen desorption temperature and improved the dehydrogenation kinetics of MgH_2, especially for Sample ① prepared at 0.035 mm/min. The optimized catalytic performance can be explained by two key factors. Firstly, polystyrene decomposition during high-temperature calcination generates gas bubbles, which not only promote the partial conversion of Nb_2O_5 to NbC but also inhibit the aggregation of heterojunction particles, ensur-

ing uniform dispersion of active sites in the carbon fiber framework. Secondly, high-energy ball milling facilitates the uniform mixing of the catalyst with MgH_2, breaks the surface passivation layer of MgH_2, exposes fresh active surfaces, increases lattice defects and internal stress, and shortens the hydrogen diffusion path, thereby reducing the dehydrogenation activation energy of MgH_2.

Compared with pure ball-milled MgH_2, the initial desorption temperature of Sample ① decreased by 52.1˚C, and the peak desorption temperature dropped by 29.1˚C, verifying the remarkable synergistic catalytic effect of Nb_2O_5-NbC heterojunctions. The slight decrease in hydrogen desorption capacity of catalyzed samples is mainly due to the mass fraction of the catalyst in the composite, which does not affect the overall catalytic superiority of the material.

Despite the enhanced dehydrogenation performance of MgH_2 catalyzed by Nb_2O_5-NbC/CNF-PS, there are still limitations in this study. The hydrogen adsorption performance and cycling stability of the composite have not been systematically investigated, and the long-term catalytic durability under repeated hydrogen absorption-desorption cycles remains to be verified. In future work, the catalyst dosage will be further optimized, and the cycling performance and hydrogen absorption kinetics will be tested in depth. Additionally, *in-situ* characterization techniques will be adopted to reveal the catalytic mechanism of Nb_2O_5-NbC heterojunctions on MgH_2 at the atomic scale, providing theoretical support for the development of high-performance Mg-based hydrogen storage materials.

5. Conclusions

In summary, this work employed electrospinning to *in-situ* construct Nb_2O_5-NbC Heterojunctionswithin carbon nanofiber (CNF) matrices via polystyrene (PS) introduction, aiming to enhance the hydrogen storage performance of Mg-based materials. Results indicate that the synthesized Nb_2O_5-NbC/CNF-PS nanocomposite exhibits a low initial hydrogen desorption temperature of 293.6˚C and a high hydrogen storage capacity of 6.48 wt.%. While ball-milled MgH_2 begins desorption at 346.2˚C, the MgH_2-10 wt.% (Nb_2O_5-NbC/CNF-PS) composite releases over 4.89 wt.% H_2 at this temperature, with its initial desorption temperature reduced by 52.6˚C.

Scanning electron microscopy (SEM) revealed that decreasing electrospinning speed reduces carbon nanotube diameter and promotes uniform distribution of Nb_2O_5-NbC Heterojunctionson CNFs. Based on the above results, it can be demonstrated that the Nb_2O_5-NbC heterojunctions used as catalysts can effectively improve the hydrogen storage properties of MgH_2. This PS-assisted synthesis strategy for Nb_2O_5-NbC/CNF offers new insights into scalable and cost-effective industrial production of carbon-based materials.

Funding

This work was financially supported by the 13th Graduate Education Innovation Fund of Wuhan Institute of Technology (No. CX2021023).

Conflicts of Interest

The author declares no conflicts of interest regarding the publication of this paper.

References

[1] Schlapbach, L. and Züttel, A. (2001) Hydrogen-Storage Materials for Mobile Applications. *Nature*, **414**, 353-358. https://doi.org/10.1038/35104634

[2] Tollefson, J. (2010) Hydrogen Vehicles: Fuel of the Future? *Nature*, **464**, 1262-1264. https://doi.org/10.1038/4641262a

[3] Yang, J., Sudik, A., Wolverton, C. and Siegel, D.J. (2010) High Capacity Hydrogenstorage Materials: Attributes for Automotive Applications and Techniques for Materials Discovery. *Chemical Society Reviews*, **39**, 656-675. https://doi.org/10.1039/b802882f

[4] Webb, C.J. (2015) A Review of Catalyst-Enhanced Magnesium Hydride as a Hydrogen Storage Material. *Journal of Physics and Chemistry of Solids*, **84**, 96-106. https://doi.org/10.1016/j.jpcs.2014.06.014

[5] Hanada, N., Ichikawa, T. and Fujii, H. (2005) Catalytic Effect of Nanoparticle 3D-Transition Metals on Hydrogen Storage Properties in Magnesium Hydride MgH_2 Prepared by Mechanical Milling. *The Journal of Physical Chemistry B*, **109**, 7188-7194. https://doi.org/10.1021/jp044576c

[6] Dobrovolsky, V.D., Ershova, O.G., Solonin, Y.M., Khyzhun, O.Y. and Paul-Boncour, V. (2008) Influence of TiB_2 Addition Upon Thermal Stability and Decomposition Temperature of the MgH_2 Hydride of a Mg-Based Mechanical Alloy. *Journal of Alloys and Compounds*, **465**, 177-182. https://doi.org/10.1016/j.jallcom.2007.10.125

[7] Huot, J., Pelletier, J.F., Lurio, L.B., Sutton, M. and Schulz, R. (2003) Investigation of Dehydrogenation Mechanism of MgH_2-Nb Nanocomposites. *Journal of Alloys and Compounds*, **348**, 319-324. https://doi.org/10.1016/s0925-8388(02)00839-3

[8] Zhang, L., Nyahuma, F.M., Zhang, H., Cheng, C., Zheng, J., Wu, F., *et al.* (2023) Metal Organic Framework Supported Niobium Pentoxide Nanoparticles with Exceptional Catalytic Effect on Hydrogen Storage Behavior of MgH_2. *Green Energy & Environment*, **8**, 589-600. https://doi.org/10.1016/j.gee.2021.09.004

[9] Ma, T., Isobe, S., Wang, Y., Hashimoto, N. and Ohnuki, S. (2013) Nb-Gateway for Hydrogen Desorption in Nb_2O_5 Catalyzed MgH_2 Nanocomposite. *The Journal of Physical Chemistry C*, **117**, 10302-10307. https://doi.org/10.1021/jp4021883

[10] Wen, X., Liang, H., Zhao, R., Hong, F., Shi, W., Liu, H., *et al.* (2022) Regulation of the Integrated Hydrogen Storage Properties of Magnesium Hydride Using 3D Self-Assembled Amorphous Carbon-Embedded Porous Niobium Pentoxide. *Journal of Materials Chemistry A*, **10**, 16941-16951. https://doi.org/10.1039/d2ta04700d

[11] Zhang, X., Zhang, X., Zhang, L., Huang, Z., Yang, L., Gao, M., *et al.* (2023) Nb_2O_5 Nanostructures as Precursors of Cycling Catalysts for Hydrogen Storage in MgH_2. *ACS Applied Nano Materials*, **6**, 14527-14539. https://doi.org/10.1021/acsanm.3c02685

[12] Kumar, S., Kojima, Y. and Dey, G.K. (2018) Morphological Effects of Nb_2O_5 on Mg-MgH_2 System for Thermal Energy Storage Application. *International Journal of Hydrogen Energy*, **43**, 809-816. https://doi.org/10.1016/j.ijhydene.2017.11.039

[13] Wang, K., Zhang, X., Ren, Z., Zhang, X., Hu, J., Gao, M., *et al.* (2019) Nitrogen-Stimulated Superior Catalytic Activity of Niobium Oxide for Fast Full Hydrogenation of Magnesium at Ambient Temperature. *Energy Storage Materials*, **23**, 79-87. https://doi.org/10.1016/j.ensm.2019.05.029

[14] Zhang, X., Wang, K., Zhang, X., Hu, J., Gao, M., Pan, H., *et al.* (2021) Synthesis Process and Catalytic Activity of Nb_2O_5 Hollow Spheres for Reversible Hydrogen Storage of MgH_2. *International Journal of Energy Research*, **45**, 3129-3141. https://doi.org/10.1002/er.6006

[15] Wang, X., Liu, M., Tian, T., Liu, F., Wang, J., Li, J., *et al.* (2025) Fibrous V/Nb Bimetallic Oxides with Remarkable Catalytic Effect on Hydrogen Storage Properties of MgH_2. *International Journal of Hydrogen Energy*, **97**, 1168-1176. https://doi.org/10.1016/j.ijhydene.2024.12.021

[16] Zhang, J., Hou, Q., Chang, J., Zhang, D., Peng, Y. and Yang, X. (2021) Improvement of Hydrogen Storage Performance of MgH_2 by $MnMoO_4$ Rod Composite Catalyst. *Solid State Sciences*, **121**, Article ID: 106750. https://doi.org/10.1016/j.solidstatesciences.2021.106750

[17] Cao, Z., Guo, J., Chen, S., Zhang, Z., Shi, Z., Yin, Y., *et al.* (2021) *In Situ* Synthesis of an Ultrafine Heterostructural Nb_2O_5-NbC Polysulfide Promotor for High-Performance Li-S Batteries. *Journal of Materials Chemistry A*, **9**, 21867-21876. https://doi.org/10.1039/d1ta05657c

[18] Zhang, L., Wang, K., Liu, Y., Zhang, X., Hu, J., Gao, M., *et al.* (2021) Highly Active Multivalent Multielement Catalysts Derived from Hierarchical Porous $TiNb_2O_7$ Nanospheres for the Reversible Hydrogen Storage of MgH_2. *Nano Research*, **14**, 148-156. https://doi.org/10.1007/s12274-020-3058-4

[19] Meng, Y., Ju, S., Chen, W., Chen, X., Xia, G., Sun, D., *et al.* (2022) Design of Bifunctional Nb/V Interfaces for Improving Reversible Hydrogen Storage Performance of MgH_2. *Small Structures*, **3**, Article ID: 2270030. https://doi.org/10.1002/sstr.202270030

[20] Ren, L., Zhu, W., Zhang, Q., Lu, C., Sun, F., Lin, X., *et al.* (2022) MgH_2 Confinement in MoF-Derived N-Doped Porous Carbon Nanofibers for Enhanced Hydrogen Storage. *Chemical Engineering Journal*, **434**, Article ID: 134701. https://doi.org/10.1016/j.cej.2022.134701

[21] Liu, M., Zhao, S., Xiao, X., Chen, M., Sun, C., Yao, Z., *et al.* (2019) Novel 1D Carbon Nanotubes Uniformly Wrapped Nanoscale MgH_2 for Efficient Hydrogen Storage Cycling Performances with Extreme High Gravimetric and Volumetric Capacities. *Nano Energy*, **61**, 540-549. https://doi.org/10.1016/j.nanoen.2019.04.094

[22] Kajiwara, K., Sugime, H., Noda, S. and Hanada, N. (2022) Fast and Stable Hydrogen Storage in the Porous Composite of MgH_2 with Nb_2O_5 Catalyst and Carbon Nanotube. *Journal of Alloys and Compounds*, **893**, Article ID: 162206. https://doi.org/10.1016/j.jallcom.2021.162206

[23] Lan, Z., Fu, H., Zhao, R., Liu, H., Zhou, W., Ning, H., *et al.* (2022) Roles of *in Situ*-Formed NbN and Nb_2O_5 from N-Doped Nb_2C Mxene in Regulating the Re/Hydrogenation and Cycling Performance of Magnesium Hydride. *Chemical Engineering Journal*, **431**, Article ID: 133985. https://doi.org/10.1016/j.cej.2021.133985

[24] Cao, Z.X., Guo, J., Chen, S.G., Zhang, Z.N., *et al.* (2021) *In-Situ* Synthesis of Ultrafine Heterostructural Nb_2O_5-NbC Polysulfide Promoter for High-Performance Li-S Batteries. *Journal of Materials Chemistry A*, **9**, 21867-21876.